C. R. Geoscience 348 (2016) 551–560

Contents lists available at ScienceDirect

Comptes Rendus Geoscience

www.sciencedirect.com

Space Physics

Mineralogical changes upon heating in the Millbillillie meteorite: Implications for paleointensity determination in Apollo samples

Cécile Cournède [a,*], Ian Garrick-Bethell [a,b], Robert S. Coe [a], Maxime Le Goff [c], Yves Gallet [c]

[a] Department of Earth and Planetary Sciences, University of California, 1156, High Street, CA 95064 Santa Cruz, USA
[b] School of Space Research, Kyung Hee University, 17104 Yongin, Kyungki, Korea
[c] Institut de Physique du Globe de Paris, Sorbonne Paris Cité, Université Paris Diderot, UMR CNRS 7154, 75005 Paris, France

ARTICLE INFO

Article history:
Received 5 October 2016
Accepted after revision 5 October 2016
Available online 11 November 2016

Handled by Vincent Courtillot

Keywords:
Paleointensity recovery
Thermal method
Mineralogical changes
Sulfides
Millbillillie meteorite
Apollo samples

ABSTRACT

Measuring the intensity of the Moon's ancient magnetic field is an important goal of lunar sample analysis. Paleointensity estimates using thermal methods (Thellier–Thellier) raise the problem of sample alteration, especially for lunar samples carrying sulfides. To address this problem, we made real-time measurements of sample magnetization during heating with a three-axis vibrating sample magnetometer (the Triaxe, LeGoff and Gallet, 2004), in the hope that rapid heating would minimize alteration (Coe et al., 2014). We studied the Millbillillie meteorite, which has a lunar-like mineralogy. We find that after repeated heating phases to ~600 °C, we form pyrrhotite, magnetite, and magnetic phases with low (200–270 °C) Curie temperatures. These low-temperature phases appear after pyrrhotite has apparently been destroyed by subsequent heating phases, and their mineralogy is unknown. These results have implications for the paleomagnetic study of any extraterrestrial samples with even small amounts of sulfides, and further experiments are required to understand them.

1. Introduction

One of the biggest outstanding questions in lunar science is the timing and origin of the Moon's ancient magnetic field. Paleomagnetic investigations of Apollo samples have returned paleointensity estimates ranging from 0.1 up to 120 μT (Weiss and Tikoo, 2014 for a review), reflecting a possibly complex and variable dynamo history. Accurate paleointensities are of crucial interest, since they can help us to discriminate the nature of the field (e.g., dynamo or impact-generated field), and have implications for the geophysical models that produce such fields – e.g., traditional thermal convection, or more exotic tidally-stirred dynamos (Dwyer et al., 2011).

When a rock carrying ferromagnetic minerals cools from high temperature within a field, it acquires a thermal remanent magnetization (TRM). To estimate the intensity of the field (paleointensity) responsible for this TRM, the most trusted methods are thermal ones (e.g., Thellier & Thellier, 1959), since they mimic the same process by which the rock acquired its remanence. The basic principle of such methods is to compare the specimen's natural TRM with that of an artificial TRM acquired in a laboratory field of known intensity (Dunlop, 2011). Such methods have been applied to lunar rocks with often poor results (Chowdhary et al., 1987; Lawrence et al., 2008; Pearce et al., 1976; Suavet et al., 2014). Indeed, upon heating, mineralogical alteration generates new phases and the acquisition of parasitic magnetization that prevents reliable paleointensity estimates in most lunar samples.

* Corresponding author.
E-mail address: ccourned@ucsc.edu (C. Cournède).

http://dx.doi.org/10.1016/j.crte.2016.10.001
1631-0713/

To deal with the problem of alteration, methods that do not involve heating have been developed to estimate paleointensity. They are based on the sample's acquisition of anhysteretic remanent magnetization (ARM) (Markert and Heller, 1972; Tauxe et al., 1995), an artificial remanence created in the laboratory by superimposing an alternating magnetic field on a small DC field, or the acquisition of saturation isothermal remanent magnetization (sIRM) (e.g., Cisowski and Fuller, 1984; Gattacceca and Rochette, 2004), the remanence created in a rock after it has been magnetized by a saturating magnetic field at room temperature. In both cases, one compares the artificial magnetization with the natural remanent magnetization (NRM) measured in the lab by alternating field (AF) demagnetization. These methods have been extensively used on Apollo samples to estimate paleointensities (e.g., Cournède et al., 2012; Garrick-Bethell et al., 2009; Shea et al., 2012; Suavet et al., 2013; Tikoo et al., 2012, 2014). Such methods have the advantage of being non-destructive and avoid mineralogical alteration, but can be inaccurate by a factor up to ~4 (Tikoo et al., 2014; Weiss and Tikoo, 2014).

Despite the utility of room-temperature paleointensity techniques, the NRM of many lunar samples is likely a TRM, such that paleointensities are best evaluated using thermal methods. Recently, significant advances in reducing sample alteration during heating were achieved by heating in a controlled atmosphere (controlling fO_2 and using a CO_2–H_2 gas mixture, Suavet et al., 2014). These authors obtained reliable paleointensities on lunar analogs with low sulfur content. They concluded that sulfide (likely troilite)-bearing samples, such as most lunar basalts, may not be suitable for analysis when sulfur fugacity is not controlled.

To study magnetic mineral evolution during heating, previous works mainly performed rock magnetic measurements at room temperature after each heating step (e.g., hysteresis, Henry et al., 2005; Mössbauer spectroscopy, magnetic susceptibility, Li et al., 1998). In the Millbillillie meteorite magnetic susceptibility was measured after each heating step to progressively remove an imparted sIRM (Morden, 1992). In some cases, susceptibility versus temperature was investigated (Jeleńska et al., 2010; Jordanova and Jordanova, 2016). One study focused on magnetic properties of extraterrestrial material (irons to stony meteorites and some tektites) in which the main magnetic carriers were kamacite and taenite (Pechersky et al., 2012). The aim was to track and understand the mineralogical evolution upon heating using different measurement conditions for some studies and simulating natural processes for others.

The initial purpose of the present study was to take advantage of the rapid heating–cooling capability of the Triaxe instrument (LeGoff and Gallet, 2004). The Triaxe provides an order of magnitude decrease in the time required to perform a traditional thermal demagnetization, and an order of magnitude higher temperature resolution. Moreover, the Triaxe has already proven its utility by revising a previous hypothesis for extremely rapid changes in the Earth's magnetic field by reducing oxidation/reduction effects during heating (Coe et al., 2014). Unfortunately, our pilot study failed to prevent oxidation in a meteorite with a lunar-like mineralogy, Millbillillie. However, the results showed a number of interesting changes in magnetic mineralogy. Therefore, the new goal of the study became to follow and understand how such changes develop upon progressive heating. Such analysis has never been employed on extraterrestrial material. We therefore present the preliminary results obtained from Millbillillie. Our ultimate goal is to find at which temperatures which types of minerals are created, modified or destroyed, with particular attention to sulfur-bearing minerals with low Curie temperatures ($< 350\,^{\circ}C$). A better understanding of such transformations would be of valuable interest to suppress mineralogical alteration and constrain at which temperatures reliable paleointensity estimates can be obtained.

2. Methods and samples

2.1. Millbillillie meteorite

The Millbillillie meteorite is an achondrite, classified as a Ca-rich polymict eucrite (Mason et al., 1979), which is a class of meteorites that likely originated from the asteroid Vesta. It was collected soon (ten years, *Meteoritical Bulletin Database*) after its fall, thus ensuring minimal terrestrial weathering. Its magnetic mineralogy was described as follows: Fe–Ni: 0.1wt%, troilite: 0.01wt%, ilmenite: 1.3wt%, chromite: 0.4wt% (Fitzgerald, 1980). The percentage of the magnetic minerals in our samples is unknown and can be different. Previous magnetic investigations report a measurable remanence, with at least one stable component (Fu et al., 2012; Morden, 1992). One paleointensity investigation using thermal methods showed that mineralogical changes occurred at about 300 °C (Morden, 1992). The whole rock studied here (obtained from a meteorite dealer) was cut into several sub-samples. All three subsamples studied here are very fresh interior samples (no visible rust), without fusion crust (identified as 3A, 4C and 4D). Sample masses are 1.9 g, 2.1 g, and 2.2 g with natural remanent moment of $3.6{\cdot}10^{-8}$ A·m^2, $4.8{\cdot}10^{-8}$ A m^2 and $7.5{\cdot}10^{-8}$ A·m^2, respectively. Unfortunately, the NRM measured in Millbillillie appears from its AF demagnetization characteristics to be dominated by IRM (likely produced by a hand magnet after collection, data not shown here), which precluded a paleomagnetic investigation of its remanence. Further, the sample NRM was close to the limit of the instrument's sensitivity (see below). However, the meteorite is still useful for the study of oxidation and alteration processes during heating, the goal of the study.

2.2. Magnetic mineralogy and iron sulfide properties

In order to help interpret the results of our experiments, we first provide some background on iron-sulfur-bearing magnetic minerals. The pyrrhotite mineral group general formula is $Fe_{(1-x)}S$, with x ranging from 0 to 0.125. Its magnetic and mineralogic characteristics depend on the crystal structure, which is based on a NiAs structure (with A and C the axial lengths of the NiAs type-cell). As a function of composition and temperature, various ordered distributions of Fe-site vacancies produce different superstructures that are either ferrimagnetic or antiferromagnetic (Table 1 in

Pósfai et al., 2000). Overall, magnetization increases as x increases. The two extreme values for x give two end-members, troilite (FeS, 2C superstructure), which is purely antiferromagnetic and monoclinic pyrrhotite ($Fe_{0.875}S$ or Fe_7S_8, 4C), which is ferrimagnetic. In terms of magnetic transition, troilite has a Néel temperature of ~315 °C (Schwarz and Vaughan, 1972) and monoclinic pyrrhotite has a Curie temperature (T_c) between 310 and 325 °C, slightly dependent on its composition (Lotgering, 1956). Along the rest of the composition range, intermediate (stable and metastable) phases known as nC may exist. Their structure and their magnetic properties upon heating are quite complex (Schwarz and Vaughan, 1972; Wang and Salveson, 2005 for a review), which is one reason why our results are not easily interpreted. Broadly, stable intermediate phases (known as, 5C, 11C and 6C, mostly hexagonal) are purely antiferromagnetic, while metastable phases are ferrimagnetic.

2.3. The Triaxe instrument: System description and measurements methods

All measurements were performed using the Triaxe (at IPGP, Paris, France). The Triaxe is a three-axis vibrating

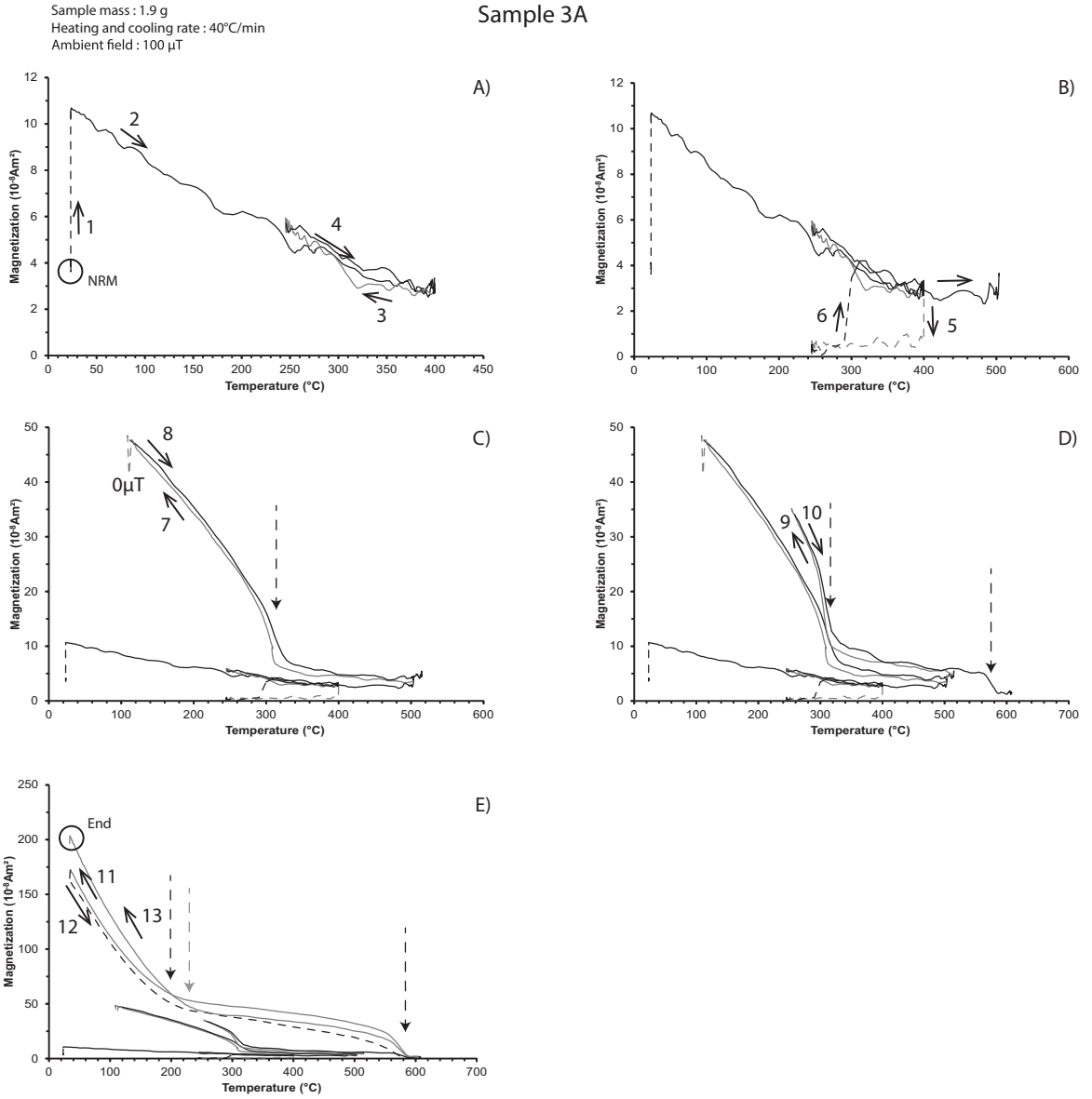

Fig. 1. Sample 3A total magnetic moment (remanent + induced) versus temperature ($M_{tot}[T]$) upon subsequent heating (black curves) and cooling (grey curves) under a field of 100 µT (solid curves) or of 0 µT (dashed curves). A-1, Field is on, 2, heating from 25 °C to 400 °C, 3, cooling from 400 °C to 250 °C, 4, heating from 250 °C to 400 °C. B-5, Cooling from 400 °C to 250 °C (in 0-µT field), 6, heating from 250 °C to 505 °C (in 0-µT field up to 300 °C). C-7, Cooling from 505 °C to 110 °C (in 0-µT field between 120 °C and 110 °C), 8, heating from 110 °C to 515 °C. D-9, Cooling from 515 °C to 255 °C, 10, heating from 255 °C to 605 °C. E-11, Cooling from 605 °C to 35 °C, 12, heating (in 0 µT field) from 35 °C to 605 °C, 13, cooling from 605 °C to 35 °C. Vertical dashed arrows point to the transitions. Black circles indicate the beginning (“NRM”) and the end (“End”) of the experiments.

sample magnetometer with a built-in furnace (Fig. 1 in LeGoff and Gallet, 2004), allowing for continuous high-temperature measurements of the remanent or induced magnetization vector. It accepts a cylindrical sample of 1-cm-diameter and 1-cm-length (volume of ~0.75 cm^3), and has a sensitivity better than 10^{-8} $A{\cdot}m^2$. This system is able to apply magnetic fields up to 200 μT in any direction, enabling acquisition of TRM during cooling. Heating-cooling rates as high as 60 °C/min are possible, thereby reaching the system's maximum temperature of 650 °C in only ~10 minutes. Paleointensity determination using the Triaxe is based on a Thellier–Thellier-like method, as explained in LeGoff and Gallet (2004).

To follow the mineralogical changes of Millbillillie upon heating, different protocols were performed on each subsample. All experiments were performed in air.

3. Results

For sample 3A, the total magnetic moment (M_{tot}) (induced + remanent [NRM]) reaches $10.6{\cdot}10^{-8}A{\cdot}m^2$ when the field is turned on (Fig. 1A). After the first heating to 400 °C, a rapid but very small increase in M_{tot} can be noticed at 320 °C upon cooling (Fig. 1A). Since the total moment (~$4{\cdot}10^{-8}$ $A{\cdot}m^2$) is close to the sensitivity of the Triaxe and the same behavior is not recovered upon the next heating to 400°, we do not consider this to be a real magnetic/mineralogical transition. This is confirmed by the following cooling–heating cycle, where the field was turned off for cooling (from 400 °C to ~250 °C), and almost no remanent magnetic moment remained. When the field was turned on again during the following heating, M_{tot} recovered its previous value and the transition at 320 °C did not appear. We therefore assume that almost no mineralogical changes develop before 400 °C. After heating to 500 °C, the $M_{tot}(T)$ cooling curve is flat between 500 °C and 320 °C and increases substantially at 320 °C (from 7 to $14{\cdot}10^{-8}$ Am^2, Fig. 1B, dashed arrow). This blocking temperature observed upon cooling (herein called unblocking temperature upon heating) is likely the Curie temperature of pyrrhotite (Fe_7S_8). At the end of the cooling, the remanent magnetic moment is 11 times higher than at the beginning of the experiment (reaching $41{\cdot}10^{-8}$ $A{\cdot}m^2$ at 120 °C when the field is turned off), suggesting the formation of new ferromagnetic minerals.

During the next heating cycle to 515 °C, the same behavior is recovered, with a sharp decrease up to ~330 °C (unblocking temperature of pyrrhotite) and a flat pattern at higher temperatures. Small differences between this heating and the prior cooling cycle could be due to the average sample temperature lagging the thermocouple temperature. The following cooling–heating cycle shows

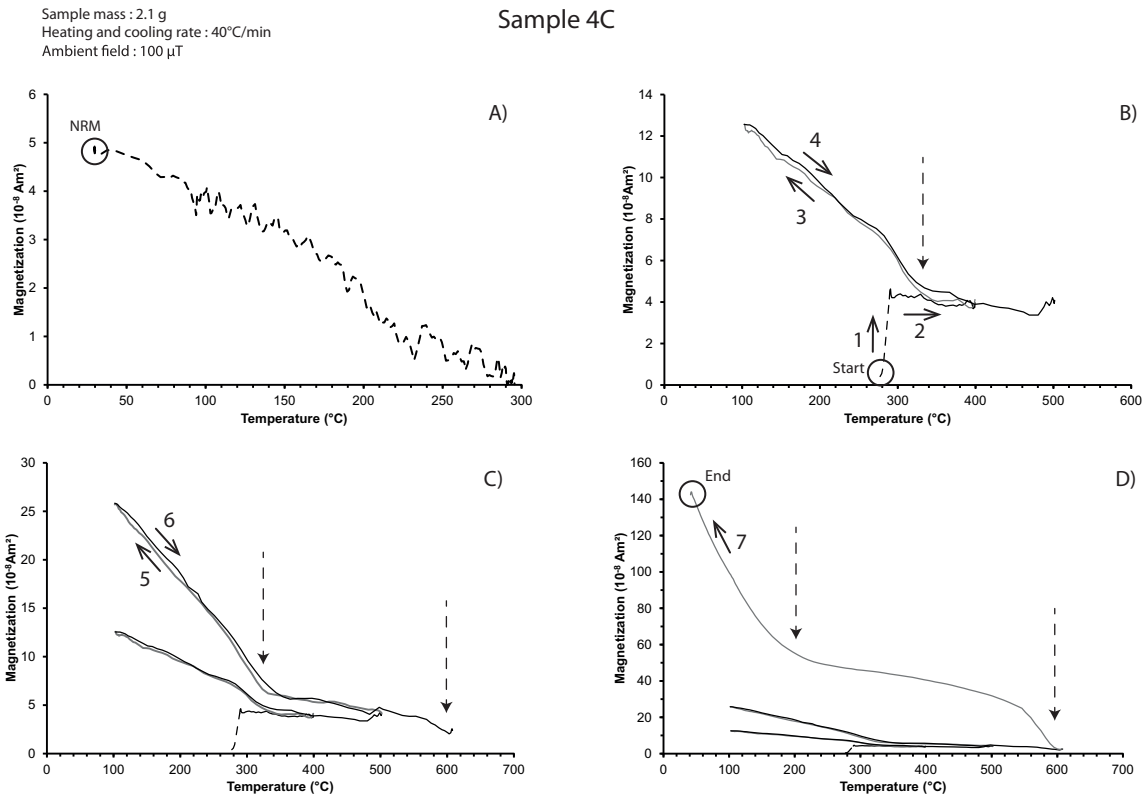

Fig. 2. Sample 4C total magnetic moment (remanent + induced) versus temperature ($M_{tot}[T]$). A. Thermal demagnetization of the NRM (likely an IRM) up to ~300 °C. Panels B to D correspond to subsequent heating (black curves) and cooling (grey curves) under a field of 100 μT (solid curves) or in 0 μT (dashed curves). B-1, Field is turned on, 2, heating from 290 °C to 400 °C, 3, cooling from 400 °C to 105 °C, 4, heating from 105 °C to 500 °C. C-5, Cooling from 500 °C to 105 °C, 6, heating from 105 °C to 610 °C. D-7, Cooling from 610 °C to 40 °C. Vertical dashed arrows point to the transitions. Black circles indicate the beginning ("Start") and the end ("End") of the progressive heating experiment.

similar behavior (Fig. 1C). However, the pyrrhotite transition at 320 °C is steeper, and there is a global increase in the total magnetic moment. The end of the heating step up to 605 °C is marked by a sharp decrease in M_{tot} around 580 °C (black dashed arrow in Fig. 1C), an unblocking temperature that is likely the Curie temperature of magnetite (Fe_3O_4). The global increase in M_{tot} mentioned previously can be explained by the formation of this new magnetic phase.

When the sample reaches a temperature of 605 °C significant changes are observed upon the subsequent cooling (Fig. 1D). Importantly, the newly (and previously) created pyrrhotite is not recovered, while a new low blocking temperature phase (LBTP) is created, as indicated by the sharp increase in the total moment at ~200 °C. The magnetite transition is still present. When the field is removed, the remanent magnetic moment remains high ($\sim 160 \cdot 10^{-8}$ A·m^2). The last heating in zero field indicates that this new LBTP is ferromagnetic. We note that through the final cooling, the LBTP transition shifted slightly, occuring at 230 °C instead of 200 °C (light gray dashed arrow in Fig. 1E. The remanent intensity at the end of the experiment is >54 times the original value at room temperature (reaching $195 \cdot 10^{-8}$ A·m^2), indicating the formation of new ferromagnetic phases.

The NRM of sample 4C is almost completely thermally demagnetized at 300 °C (Fig. 2A). Then, sample 4C exhibits similar results as those described above for sample 3A (Fig. 2B–D). However, after the first heating to 400 °C, the pyrrhotite identified previously is already created as indicated by the slight increase in M_{tot} from 4 to $12 \cdot 10^{-8}$ A·m^2 between 320 °C and room temperature during the cooling step (Fig. 2B). This observation challenges the conclusion made for sample 3A that no mineralogical changes operate before 400 °C (see above). This aspect will be discussed later (Section 4.4). When the temperature reaches 500 °C, a sharper transition marks the presence of pyrrhotite upon cooling and an increase in total magnetic moment occurs (Fig. 2C), as observed for sample 3A. This increase was associated with magnetite growth, but its presence here is not as evident as in sample 3A (M_{tot} decreases only from 4 to $2 \cdot 10^{-8}$ A·m^2 between 570 and 610 °C through the heating to 610 °C). Finally, as in 3A, the last cooling step is characterized by three majors features; a large 29-fold increase in M_{tot} (to $145 \cdot 10^{-8}$ A·m^2) at the end, the disappearance of the pyrrhotite and the presence of magnetite, plus the appearance of the LBTP (Fig. 2D).

In sample 4D, thermal demagnetization shows that less than 1% of the NRM remains after 400 °C (Fig. 3A). After heating to 610 °C, two phases are evidenced (magnetite + LBTP) as previously observed for 3A and 4C. This direct heating to high temperature has apparently avoided the formation of pyrrhotite. Moreover, we note that the LBTP transition occurs at a higher temperature (270 °C) (Fig. 3B).

While some discrepancies are observed between the three studied samples, a global pattern of the mineralogical changes that occur can be depicted (Fig. 4). The initial magnetic assemblage is almost stable up to a temperature ranging from 300 to 400 °C. Above this temperature, pyrrhotite transiently appears, followed by magnetite. Both phases coexist when a temperature of 600 °C is reached. Above, or maybe earlier, the LBTP forms while pyrrhotite disappears and magnetite is still present.

4. Discussion of mineralogical changes

4.1. Pyrrhotite formation

In agreement with a previous study (Morden, 1992), the Millbillillie meteorite magnetization increased by the end of heating experiments, indicating that mineralogical changes took place.

Among those changes, the first phase created is interpreted to be pyrrhotite, based on the transition observed at 320 °C. In the following, we will discuss three ways in which this mineral can be formed.

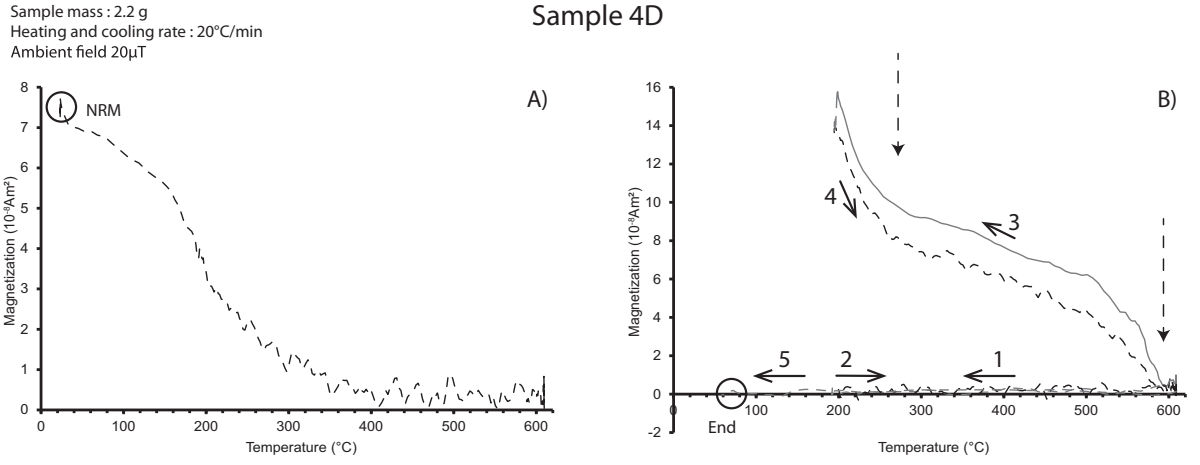

Fig. 3. Sample 4D total magnetic moment (remanent + induced) versus temperature ($M_{tot}[T]$) upon heating (black curves) and cooling (grey curves). A. Thermal demagnetization of the NRM (likely an IRM) up to 610 °C. B-1, cooling in 0-µT field from 610 °C to 200 °C, 2, heating in 0-µT field from 200 °C to 610 °C, 3, cooling in 20-µT field from 610 °C to 200 °C, 4, heating in 0-µT field from 200 °C to 610 °C, 5, cooling in 0-µT field from 610 °C to 25 °C. Vertical dashed arrows point to the transitions. Black circles indicate the beginning ("NRM") and the end ("End") of the experiments.

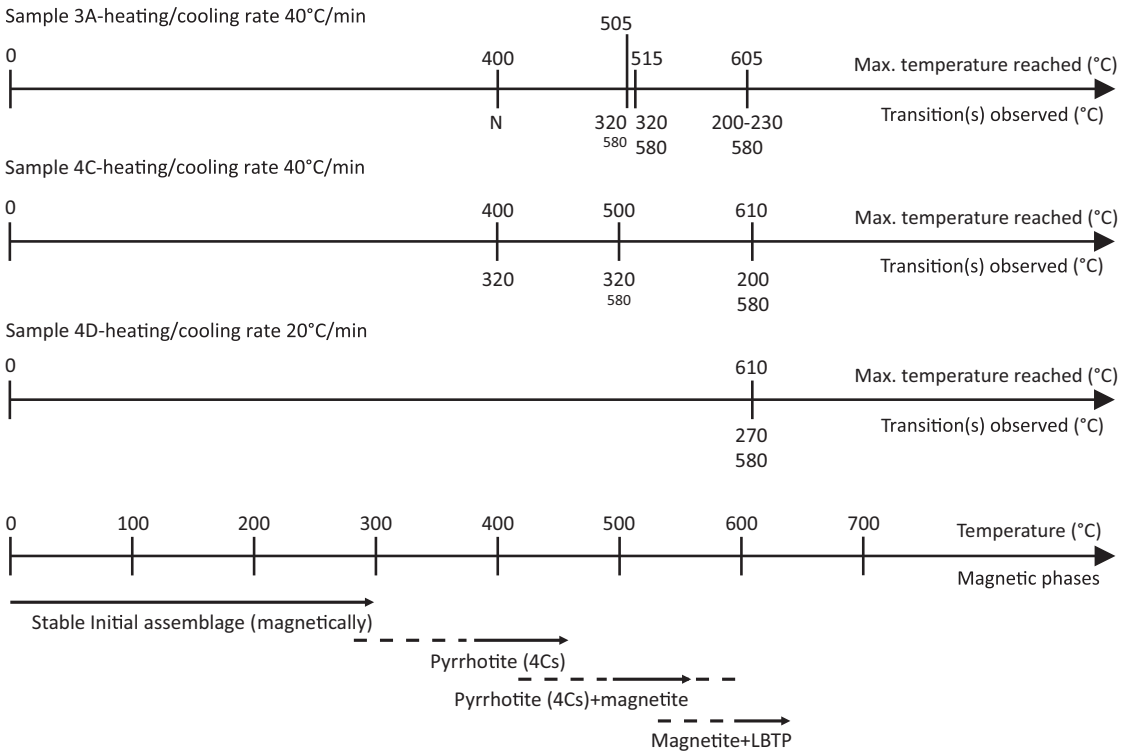

Fig. 4. For each Millbillillie subsample, the temperatures reached are indicated above and the magnetic transitions observed upon the next cooling–heating cycle are indicated below. "N" indicates that no changes are observed. Small fonts are used when the transition is small and just starts to be apparent. The temperature line at the bottom summarizes the mineralogical changes that operate after reaching the temperature shown. Solid arrows indicate where mineralogical changes are effective, with the dashed part indicating where mineralogical changes can start to operate. "4Cs" refers to 4C pyrrhotite superstructure, in contrast to subsample "4C" (cf. section 4.1 in the text).

- Considering the initial magnetic assemblage (kamacite, Fe-Ni and troilite, FeS), the pyrrhotite behavior could be mimicked by metal–troilite intergrowth textures and, more precisely, a magnetostatic interaction between these two minerals (Chowdhary et al., 1987; Pearce et al., 1976). According to these authors, troilite is reversely magnetized in the presence of iron. Such a reversal has never been properly evidenced for troilite and iron in the literature. A reverse magnetization would require impurities or lattice defects in the troilite structure (as proposed for hematite, Néel, 1955). The presence of impurities has yet to be demonstrated in Millbillillie and lattice defects may form by the thermal processes. However, the latter would likely have led to the second proposition (see below).
- Alternately, since pyrrhotite is the iron-deficient end-member of the iron sulfide solid solution, pyrrhotite (4C superstructure = 4Cs) may be produced from cation vacancies in the troilite structure created through iron liberation. To corroborate this explanation, reduction and the decomposition of troilite into iron (and possibly pyrrhotite) was observed when lunar samples were heated in controlled atmosphere (Watson et al., 1974) and in vacuum (Larson, 1978). Moreover, formation of pyrrhotite from troilite has been invoked in lunar samples to explain susceptibility variations upon heating in air (Collinson et al., 1973).
- Finally, another way to explain pyrrhotite formation could be found in the possibly complex structural forms of the iron sulfide present before heating. For example, Nakazawa and Morimoto (1971) synthesized iron sulfides of the pyrrhotite group mineral. For a composition of $Fe_{0.95}S$ (very close to that of pure troilite), they obtained two structure types, 2C (FeS) and 6C ($Fe_{11}S_{12}$, antiferromagnetic, Fig. 5). It was confirmed later that, for $x \geq 0.05$, the Fe–S system cools into a two-phase region, where the troilite phase coexists with a hexagonal phase (Li and Franzen, 1996a). The 2C + 6C mixture was then heated to 292 °C with a constant flow of heated nitrogen gas, and subsequently cooled. The resulting phase was 4.5 C, a magnetic metastable intermediate pyrrhotite with a non-integer C dimension superstructure. Regarding this experiment, and in order to explain our results, we suggest that the troilite phase identified in the initial mineralogic assemblage could be a mixture of iron sulfide structures, likely troilite + an intermediate phase. Such a mixture may convert upon heating into pyrrhotite (equal or close to 4Cs) with an atomic percentage iron comprised between 46.7 and 47% (Fig. 5, light grey zone). Curie temperatures for this range of composition are consistent with the transition, we observed at ~320 °C. This mechanism has never been observed previously.

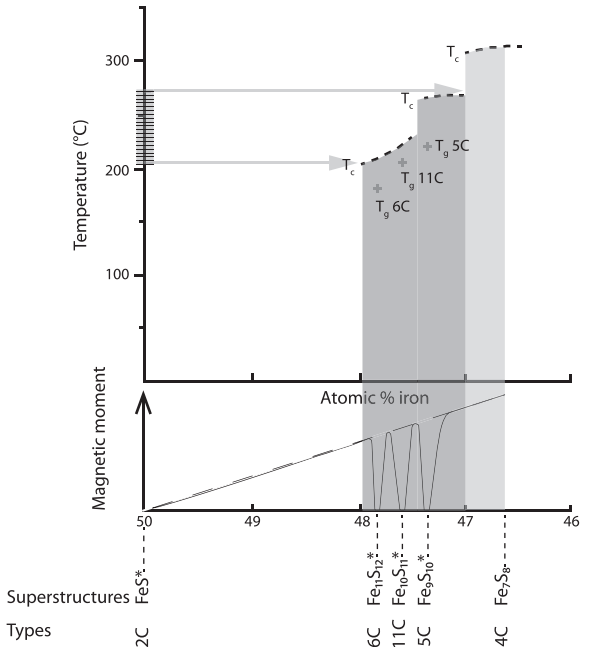

Fig. 5. Magnetic phase diagram for synthetic pyrrhotites annealed at 144 °C (simplified from Schwarz and Vaughan, 1972), curie temperatures (T_c, dark dashed lines) and gamma transition (T_g) are reported (light grey cross). T_c corresponds to the ferromagnetic-to-paramagnetic ordering, T_g corresponds to the antiferromagnetic-to-ferrimagnetic ordering. Below is the periodic pattern of the relationship between iron-sulfide composition and net magnetic moment (adapted from Wang and Salveson, 2005). Superstructures and types are indicated below the graphs. Antiferromagnetic superstructures are indicated with *. The light grey zone indicates the range of composition for which pyrrhotite has a Curie temperature close to ~320 °C. The horizontal hatched zone on the *Y*-axis represents the low blocking temperature range observed in our experiments. The dark grey zone indicates the range of composition corresponding to these temperatures.

Considering the poor constraints, we have concerning the initial structure of troilite, we favor the second hypothesis to account for the appearance of pyrrhotite.

4.2. Magnetite growth

The second phase created, when a temperature of 500 °C is reached, is magnetite. Insights into the formation of magnetite can be obtained from studies on terrestrial rocks. For instance, Li et al., 1998 observed an enhancement of susceptibility in sandstone and siltstone samples between 400 and 650 °C, which they explained by the transformation of trace amount of sulfides into magnetite/maghemite and ultimately hematite. Similarly, in Devonian sediments from Algeria, Aïfa, 1993 inferred from thermomagnetic curves that mineralogical changes between 500 °C and 550 °C were attributable to sulfides (possibly of pyrrhotite type) transforming into magnetite. Such conversions have been previously documented (Bennet and Graham, 1980; Soffel, 1977). More recently, the magnetic monitoring of individual pyrrhotites performed during stepwise thermal demagnetization under air showed a progressive oxidation via magnetite to hematite for a temperature > 500 °C (Dekkers, 1990). Considering our results, the formation of magnetite through the breakdown of troilite reported in ordinary chondrites (Collinson, 1987) may be explained as follows for Millbillillie: upon heating the initial troilite evolves into a transient pyrrhotite (4Cs) that oxidizes into magnetite. Besides sulfides, kamacite oxidation can also lead to magnetite formation (Suavet et al., 2014). Our observations are in agreement with the previous study on Millbillillie which reported that above 500 °C Fe starts to oxidize (Morden, 1992).

4.3. LBTP appearance

The most striking feature after heating to 605–610 °C was the disappearance of pyrrhotite and the appearance of the LBTP (at 200-270 °C upon cooling). At first, one could interpret this change as the breakdown of pyrrhotite into a new phase of the Fe–S system (concomitantly with its oxidation into magnetite). For example, it has been shown that after heating to high temperature (600 °C), mostly antiferromagnetic intermediate pyrrhotite types (5C, 11C, 6C) remain (Li and Franzen, 1996b). The problem is that such phases are ferrimagnetic only between the gamma transition (T_g, which corresponds to the antiferromagnetic to ferrimagnetic ordering) (150–230 °C) and T_c (205-270 °C) (Fig. 5). In this case, one would expect an increase in magnetization after T_g and a rapid drop at T_c. Such a change is not observed in our results. However, the LBTP transition (200–270 °C) overlaps with Curie temperatures defined for metastable ferrimagnetic phases with an atomic iron percentage ranging from 47 to 48% (dark grey in Fig. 5). This would mean that the pyrrhotite (4Cs) formed previously is a transient phase (unstable at high temperatures), which transforms back into such an intermediate ferrimagnetic metastable form.

The shift of the LBTP from 200 to 230 °C observed in sample 3A during the two last cooling phases (from 605 °C) may be related to progressive equilibration of partially altered phases upon subsequent heating to this maximum temperature (605 °C, Fig. 4). This could be the case if oxidation did not occur homogeneously throughout the volume of the pyrrhotites.

It is noteworthy that the LBTPs are observed at much lower temperatures (~200–230 °C) in samples 3A and 4C than for 4D (270 °C). In that case, beyond equilibration issues (above), the difference could result from different cooling rates (40°/min for sample 3A and 4C or 20 °C/min for sample 4D). It appears that a faster cooling rate may produce a lower transition temperature. As observed for heating above 450 °C in pyrrhotite (Dekkers, 1990) and in titanomagnetite (Bowles et al., 2013), a faster cooling rate might freeze in more disordered states with lower Curie temperatures.

Finally, it is plausible that other minerals with low blocking temperature may account for the results we obtained. For definite conclusions, more experimental data are needed to explain the LBTP.

4.4. Implications for Millbillillie paleomagnetism

In our samples, mineralogical changes begin before (in sample 4C) or slightly after (in sample 3A) a temperature of

400 °C was reached (Fig. 4). A previous study indicated that mineralogical changes start to operate at 300 °C in Millbillillie (increase in susceptibility) (Morden, 1992). We thus conclude that the initial assemblage of magnetic minerals is stable up to a temperature between 300 and 400 °C. One thermal demagnetization study of the NRM in Millbillillie reported three stable components; a low, a medium and a high temperature component (Fu et al., 2012). This latter was defined between 135 and 540 °C. Our observations suggest that caution should be taken in interpreting this component.

Millbillillie is a polymict breccia with some clast-rich and clast-poor regions resulting in a layered structure (Fitzgerald, 1980). Small-scale variations may occur in our subsamples, such that different mineralogies may produce different behavior upon heating. It is also possible that the protocol followed can also influence the observed transitions (Fig. 4). In sample 3A, the progressive heating–cooling sequence was started right after the NRM was measured, while in sample 4C low-temperature (to 300 °C) measurements (results not presented here) were performed after the NRM thermal demagnetization to 300 °C (Fig. 2A), and before the full protocol (Fig. 2B–D). These prior analyses below 300 °C in sample 4C may have acted as a precursor of the alteration, destabilizing the initial mineralogical assemblage and leading to formation of pyrrhotite at a lower maximum heating temperature than in sample 3A. Similarly, in sample 3A, magnetite growth could have been accelerated by the double heating it experienced to ~500 °C (505 and then 515 °C). Alternately, the magnetite growth in3A could just be the result of the progressive increase of the maximum temperature reached. It is still uncertain if the result of heating is more affected by the maximum temperature reached (as shown for a carbonaceous chondrite by Nakato et al., 2016 and in sample 4D) or by the number of heating–cooling steps performed.

Kamacite, one of the main magnetic carriers in Millbillillie, is not evidenced in our results. It might be expected that if the Triaxe could reach higher temperatures, a poorly defined kamacite Curie point (~780 °C) would have occurred (as observed in Morden, 1992), assuming that all kamacite is not oxidized before that point.

5. Implication for lunar samples

We have shown that for Millbillillie a very small amount of iron sulfide may play a large role in the magnetic behavior upon heating. The mineralogical assemblage in Millbillillie is comparable to that of some Apollo samples. Therefore, when thermal methods are used for paleointensity determinations on lunar samples (containing troilite) a similar scenario might be expected. In the following, we will discuss this possibility through the example of an extensively studied Apollo sample, 62235. The lunar impact melt breccia 62235 contains kamacite (1.2 vol%), troilite (0.1 vol%), and ilmenite (2.8vol%) (Vaniman and Papike, 1980). Its age was found to be 3.872 ± 0.032 Ga ($^{39}Ar/^{40}Ar$, Norman et al., 2006). Paleomagnetic investigations reported two successful Thellier–Thellier experiments (Collinson et al., 1973; Sugiura and Strangway, 1983), and one that failed (Pearce et al., 1976). The remanence was shown to be mostly directionally stable up to 500 °C. Mineralogical changes were monitored by measuring IRM after each heating, indicating that it was stable up to 600 °C (Collinson et al., 1973). A fourth study found that 62235 can record a reliable paleointensity up to ~450 °C, after which alteration may begin, leaving any high-temperature component uninterpretable (Lawrence et al., 2008). The paleointensity estimated from the low-temperature component was 92 μT, but concerns about the primary origin and the nature of this component were raised (Lawrence et al., 2008). Furthermore, high paleointensity is difficult to reconcile with theories of lunar dynamo action at ~3.9 Ga (Weiss and Tikoo, 2014).

The Triaxe could be helpful for elucidating the magnetic history of 62235, given its ~10-fold increase in temperature resolution compared to other Thellier–Thellier systems. One aim would be to resolve the low- and high-temperature components identified by Lawrence et al., 2008, this time using AF demagnetization to remove the putative IRM the sample received, prior to heating. The second goal would be to retrieve a more reliable paleointensity, possibly correcting for the effects of sulfur phase transformations, which were suggested for this sample by Pearce et al. (1976). Further experiments with Millbillillie and other meteorites should help clarify the extent to which one can correct for such transformations.

6. Conclusion

We performed stepwise heating on the Millbillillie meteorite using the Triaxe. The original magnetic assemblage remains stable up to ~300 °C. Above this temperature, new ferrimagnetic phases are identified. We propose that the initial troilite breaks down into pyrrhotite (4Cs) between 300 and 400 °C. This phase and plausibly kamacite convert into magnetite beginning at ~500 °C, and when a temperature of 600 °C is reached a new phase with low blocking (unblocking) temperature (LBTP) is created. Further studies are needed to determine exactly the nature of this phase. Some differences of behavior were observed between subsamples. This may be attributed to the brecciated nature of Millbillillie for some samples, and to different measurement conditions for others (e.g., heating–cooling rates).

Further studies should be conducted on additional Millbillillie samples including:

- progressive stepwise heating in order to better constrain the temperature at which alteration starts;
- different heating–cooling rates and steps to evaluate if such parameters have an influence on the temperature at which transitions occur;
- complementary magnetic property measurements after each heating/cooling step, such as magnetic susceptibility and/or mineralogical analysis.

Tests on some lunar samples (e.g., 62235) should also be considered. The Triaxe is a powerful tool for paleointensity determination in terrestrial rocks and

archaeological artefacts, and has been shown to be very useful for following mineralogical alterations in Millbillillie.

Acknowledgements

Cécile Cournède, Ian Garrick-Bethell, and Robert Coe acknowledge support from the NASA Solar System Workings Program (grant # NNX15AH47G). This work was partially supported by the BK21 plus program through the National Research Foundation (NRF), funded by the Ministry of Education of Korea and the Louis Gentil–Jacques Bourcart award from the French ''Académie des sciences''. The first author was invited by the chief editor to propose a paper, as the recipient of one of the Academy of Sciences prizes for 2015. The authors also thank Pierre Rochette for his helpful comments. The chief editor thanks Pierre Rochette for his review of this invited paper.

References

Aïfa, T., 1993. Different styles of remagnetization in Devonian sediments from the north-western Sahara (Algeria). Geophys. J. Int. 115, 529–537.

Bennet, C.E.G., Graham, J., 1980. New observations on natural pyrrhotite. Part III. Thermomagnetic experiments. Am. Mineral. 65, 800–807.

Bowles, J.A., Jackson, M.J., Berquó, T.S., Sølheid, P.A., Gee, J.S., 2013. Inferred time- and temperature-dependent cation ordering in natural titanomagnetites. Nat. Commun. 4, 1916.

Chowdhary, S.K., Collinson, D.W., Stephenson, A., Runcorn, S.K., 1987. Further investigations into lunar paleointensity determinations. Phys. Earth Planet. Inter. 49, 133–141.

Cisowski, S.M., Fuller, M., 1984. Lunar paleointensities via the IRMs normalization method and the early magnetic history of the moon. In: Origin of the moon; Proceedings of the Conference, Kona, HI, Lunar and Planetary Institute, pp. 411–424.

Coe, R., Jarboe, N., Le Goff, M., Petersen, N., 2014. Demise of the rapid-field-change hypothesis at Steens Mountain: the crucial role of continuous thermal demagnetization. Earth Planet. Sci. Lett. 400, 302–312.

Collinson, D.W., 1987. Magnetic properties of the Olivenza meteorite-possible implications for its evolution and an early solar system magnetic field. Earth Planet. Sci. Lett. 84, 369–380.

Collinson, D.W., Stephenson, A., Runcorn, S.K., 1973. Magnetic properties of Apollo 15 and 16 rocks. Proc. Lunar Sci. Conf. 4, 2963.

Cournède, C., Gattacceca, J., Rochette, P., 2012. Magnetic study of large Apollo samples: Possible evidence for an ancient centered dipolar field on the Moon. Earth Planet. Sci. Lett. 331–332 (31-42).

Dekkers, M.J., 1990. Magnetic monitoring of pyrrhotite alteration during thermal demagnetization. Geophys. Res. Lett. 17, 779–782.

Dunlop, D.J., 2011. Physical basis of the Thellier-Thellier and related paleointensity methods. Phys. Earth Planet. Inter. 187, 118–138.

Dwyer, C.A., Stevenson, D.J., Nimmo, F., 2011. A long-lived lunar dynamo driven by continuous mechanical stirring. Nature 479, 212–214.

Fitzgerald, M.J., 1980. Mukera and Millbillillie-Australian achondritic meteorites. Trans. Royal Soc. South Austr. 104, 201–209.

Fu, R., Weiss, B.P., Li, L., Suavet, C., Gattacceca, J., Lima, E.A., 2012. Magnetic fields on 4 Vesta as recorded in two eucrites. Lunar Planet. Sci. Conf. 43, 1946.

Garrick-Bethell, I., Weiss, B.P., Shuster, D.L., Buz, J., 2009. Early lunar magnetism. Science 323, 356–359.

Gattacceca, J., Rochette, P., 2004. Toward a robust normalized magnetic paleointensity method applied to meteorites. Earth Planet. Sci. Lett. 227, 377–393.

Henry, B., Jordanova, D., Jordanova, N., Le Goff, M., 2005. Transformations of magnetic mineralogy revealed by difference of hysteresis loops measured after stepwise heating: Theory and case studies. Geophys. J. Int. 162, 64–78.

Jeleńska, M., Hasso-Agopsowicz, A., Kopcewicz, B., 2010. Thermally induced transformation of magnetic minerals in soil based on rock magnetic study and mössbauer analysis. Phys. Earth Planet. Inter. 179, 164–177.

Jordanova, D., Jordanova, N., 2016. Thermomagnetic behavior of magnetic susceptibility-Heating rate and sample size effects. Front. Earth Sci. 3, 90.

Larson, E.E., 1978. Degradation of lunar basalts during thermal heating in vacuum and its relation to paleointensity measurements. Lunar Planet. Sci. IX, (#633).

Lawrence, K., Johnson, C., Tauxe, L., Gee, J.S., 2008. Lunar paleointensity measurements: Implications for lunar magnetic evolution. Phys. Earth Planet. Inter. 168, 71–87.

LeGoff, M., Gallet, Y., 2004. A new three-axis vibrating sample magnetometer for continuous high-temperature magnetization measurements: applications to paleo- and archeo-intensity determinations. Earth Planet. Sci. Lett. 229, 31–43.

Li, F., Franzen, H.F., 1996a. Phase transitions in near stoichiometric iron sulfide. J. Alloys Compds 238, 73–80.

Li, F., Franzen, H.F., 1996b. Ordering, Incommensuration, and Phase Transitions in Pyrrhotite Part II: A High-Temperature X-Ray Powder Diffraction and Thermomagnetic Study. J. Solid State Chem. 126, 108–120.

Li, Z.X., Dobson, J., Chen, Z., Chang, W.J., St. Pierre, T.G., 1998. Multimodal investigation of thermally induced changes in magnetic fabric and magnetic mineralogy. Geophys. J. Int. 135, 988–998.

Lotgering, F.K., 1956. On the ferrimagnetism of some sulphides and oxides. Philips Res. Rep. 11, 190–249.

Markert, H., Heller, F., 1972. Determination of Palaeointensities of the Geomagnetic Field from Anhysteretic Remanent Magnetization Measurements. Phys. Status Solidi 14, K47.

Mason, B., Jarosewich, E., Nelen, J.A., 1979. The pyroxene plagioclase achondrites. Smithson. Contrib. Earth Sci. 22, 1059–1078.

Morden, S.J., 1992. Magnetic study of the Millbillillie (eucrite) achondrite - Evidence for a dynamo-type magnetizing field. Meteoritics 27, 560–567.

Nakato, A., Chan, Q.H.S., Nakamura, T., Kebukawa, Y., Zolensky, M.E., and Astromaterials Science Research Group, 2016. Mineralogy of experimentally heated Tagish Lake. In: 47th Lunar and Planetary Science Conference. (#1218).

Nakazawa, H., Morimoto, N., 1971. Phase relations and superstructures of pyrrhotite $Fe_{1-x}S$. Mat. Res. Bull. 6, 345–358.

Norman, M.D., Duncan, R.A., Huard, J.J., 2006. Identifying impact events within the lunar cataclysmfrom ^{40}Ar-^{39}Ar ages and compositions of Apollo 16 impact melt rocks. Geochim. Cosmochim. Acta 70, 6032–6049.

Néel, L., 1955. Some theoretical aspects of rock-magnetism. Adv. Phys. 4 (14), 191–243.

Pearce, G.W., Hoye, G.S., Strangway, D.W., Walker, B.M., Taylor, L.A., 1976. Some complexities in the determination of lunar paleointensities. Proc. 7th Lunar Sci. Conf. 3271–3297.

Pechersky, D.M., Markov, G.P., Tsel'movich, V.A., Sharonova, Z.V., 2012. Extraterrestrial Magnetic Minerals. Phys. Solid Earth 48, 653–669.

Pósfai, M., Sharp, T.G., Kontny, A., 2000. Pyrrhotite varieties from the 9.1 km deep borehole of the KTB project. Am. Mineral. 85, 1406–1415.

Schwarz, E.J., Vaughan, D.J., 1972. Magnetic phase relations of pyrrhotite. J. Geomag. Geoelec. 24, 441–458.

Shea, E.K., Weiss, B.P., Cassata, W.S., Shuster, D.L., Tikoo, S.M., Gattacceca, J., Grove, T.L., Fuller, M.D., 2012. A long-lived lunar core dynamo. Science 335, 453–456.

Soffel, H., 1977. Pseudo-single-domain effect and single-domain multidomain transition in natural pyrrhotite deduced from domain structure observations. J. Geophys. 42, 351–359.

Suavet, C., Weiss, B.P., Cassata, W.S., Shuster, D.L., Gattacceca, J., Chan, L., Garrick-Bethell, I., Head, J.W., Grove, T.L., Fuller, M.D., 2013. Persistence and origin of the lunar core dynamo. Proc. Natl. Acad. Sci. U. S. A. 110, 8453–8458.

Suavet, C., Weiss, B.P., Grove, T.L., 2014. Controlled-atmosphere thermal demagnetization and paleointensity analyses of extraterrestrial rocks. Geochem. Geophys. Geosyst. 15, 2733–2743.

Sugiura, N., Strangway, D.W., 1983. Magnetic paleointensity determination on lunar sample 62235. Lunar Planet. Sci. Conf. Proc. Part 2. A684–A690.

Tauxe, L., Pick, T., Kok, Y.S., 1995. Relative paleointensity in sediments: a pseudo-Thellier approach. Geophys. Res. Lett. 22, 2885–2888.

Thellier, E., Thellier, O., 1959. Sur l'intensité du champ magnétique terrestre dans le passé historique et géologique. Ann. Geofis. 15, 285–376.

Tikoo, S.M., Weiss, B.P., Buz, J., Lima, E.A., Shea, E.K., Melo, G., Grove, T.L., 2012. Magnetic fidelity of lunar samples and implications for an ancient core dynamo. Earth Planet. Sci. Lett. 337–338 (93-103).

Tikoo, S.M., Weiss, B.P., Cassata, W.S., Shuster, D.L., Gattacceca, J., Lima, E.A., Suavet, C., Nimmo, F., Fuller, M.D., 2014. Decline of the lunar core dynamo. Earth Planet. Sci. Lett. 404, 89–97.

Vaniman, D.T., Papike, J.J., 1980. Lunar highland melt rocks: chemistry, petrology and silicates mineralogy. Proc. Conf. Lunar Highlands Crust 271–337.

Wang, H., Salveson, I., 2005. A review on the mineral chemistry of the nonstoichiometric iron sulphide. $Fe_{1-x}S$ ($0 \leq x \leq 0.125$): polymorphs, phase relations and transitions, electronic and magnetic structures. Phase Transit. 78, 547–567.

Watson, D.E., Larson, E.E., Reynolds, R.L., 1974. Microscopic and thermomagnetic analysis of Apollo 17 breccia and basalt: Feasibility of obtaining meaningful paleointensities of the lunar magnetic field. Lunar Planet. Sci. Conf. 5, 827–829.

Weiss, B.P., Tikoo, S.M., 2014. The lunar dynamo. Science 346, 1246753-1-10.